# Self-Organization in Semiconductor Lasers with Ultrashort Optical Feedback

O. Ushakov,[1] S. Bauer,[2] O. Brox,[2] H.-J. Wünsche,[1] and F. Henneberger[1,*]

[1]*Humboldt-Universität Berlin, Institut für Physik, Newtonstrasse 15, 12489 Berlin, Germany*

[2]*Fraunhofer-Institute for Telecommunications, Heinrich-Hertz-Institut, Einsteinufer 37, 10587 Berlin, Germany*

(Received 7 August 2003; published 28 January 2004)

The dynamical behavior of a single-mode laser subject to optical feedback is investigated in the limit, when the delay time is much shorter than the period of the relaxation oscillations. Use of an integrated distributed feedback device allows us to control the feedback phase. We observe two kinds of Hopf bifurcations associated with regular self-pulsations of different frequencies.

DOI: 10.1103/PhysRevLett.92.043902 PACS numbers: 42.55.Px, 05.45.–a, 05.65.+b

The single-mode laser is a paradigm of self-organization in dissipative systems [1]. At threshold, one optical mode becomes undamped in a Hopf bifurcation, actuating a transition from incoherent to coherent emission. Optical feedback, achieved by combining the laser with an external cavity, destabilizes the continuous-wave (cw) state [2]. Fundamentally new dynamical scenarios evolve, with considerable potential for applications in optical technologies. In this Letter, we focus on the short-cavity limit, where the feedback delay ($\tau$) through the external round-trip is much shorter than the period ($\tau_R$) of the relaxation oscillations in the solitary laser. In this case, the phase shift $\phi$ induced by the external cavity determines essentially the laser dynamics. Recently, cyclic behavior leading from stable emission to regular and irregular pulse packages has been observed in an external mirror arrangement with ratios $\tau/\tau_R \approx 0.3$–$1.0$ [3]. A limited but still sizable number of cavity modes is involved in these packages. The question we address is whether this observation represents the ultimate short-cavity limit or whether other routes of self-organization still exist. A rich variety of phenomena has been predicted in general for lasers with moderately delayed optical feedback [4–8]; however, no study explicitly focusing on $\tau \to 0$ is available so far.

Distributed-feedback (DFB) semiconductor lasers exhibit single-mode cw emission up to high pump currents. After perturbation, they return to the stationary state by well-damped relaxation oscillations with a period of some 100 ps. Laser and external cavities, both with a length of about 100 $\mu$m, can be monolithically integrated in a single device [9]. In this way, the range of $\tau/\tau_R \approx 0.01$ becomes experimentally accessible. In what follows, we demonstrate that, indeed, nontrivial dynamics exists beyond pulse-package regime. Two types of Hopf bifurcations characteristic of the ultrashort cavity limit occur. They give rise to stable self-pulsations of different frequencies, associated with a single-mode or a pair of modes.

The (InGaAs)P/InP device (Fig. 1) used in this study consists of a 1.55 $\mu$m active DFB section of length $L_{DFB} = 220$ $\mu$m, embedded in an asymmetric 1.3 $\mu$m optical waveguide with an index-coupled grating on top. The adjacent passive section ($L_P = 200$ $\mu$m) is implemented by omitting the 1.55 $\mu$m layer as well as the grating. While the DFB edge is antireflection coated, the facet of the passive section is cleaved providing feedback with power reflectivity of $R \approx 0.3$. Both sections are independently biased. Injection in the passive part allows us to tune the feedback phase via free-carrier transitions. The device output was analyzed on the DFB facet by coupling it into a single-mode fiber. Optical spectra were recorded by a Czerny-Turner spectrometer with 0.015 nm resolution and an infrared camera as detector. Power spectra were acquired by an electrical spectrum analyzer (R&S FSP 9) with 40 GHz bandwidth in conjunction with an u2t photodiode of 9 ps response time. Measurements in the time domain were carried out by means of a digital 50 GHz sampling oscilloscope (HP 54120B). The temperature stabilization in all measurements is 0.05 °C.

The device features three regimes of operation. Representative spectra are summarized in Fig. 2. A single line in the optical spectrum and a flat noise floor in the power spectrum are attributes of cw emission. Self-pulsations are manifested by a distinct peak in the power spectrum and a corresponding splitting of the optical emission line into several substructures. Two different kinds of self-pulsations are observed. Pulsations of lower frequency are characterized by a closely spaced comb of optical lines. In the power spectrum, a main peak shows up at the frequency of the optical line separation, followed by a series of higher harmonics. On the contrary, for the higher-frequency pulsations, a couple of well-separated optical lines is present, again with a corresponding peak

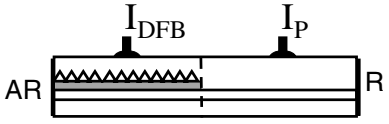


FIG. 1. Schematics of a DFB laser (left) with integrated feedback section (right). AR: antireflection coating. R: cleaved facet.

  

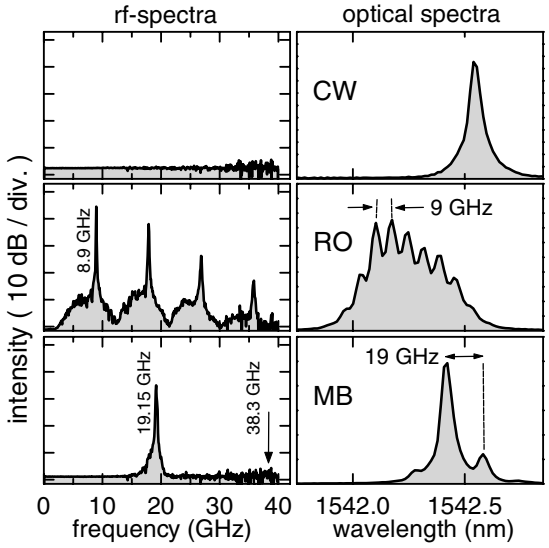


FIG. 2. Regimes of operation of the ultrashort feedback laser. Left column: power spectra; right column: optical spectra. CW: $I_{DFB} = 65$ mA, $I_P = 45$ mA; RO: $I_{DFB} = 50$ mA, $I_P = 28$ mA; MB: $I_{DFB} = 70$ mA, $I_P = 11$ mA. Note the log scale.

in the power spectrum. The absence of higher harmonics signifies here almost perfect sinusoidal behavior. For reasons that will become clear below we distinguish between both kinds of oscillatory laser output by using the terms "relaxation-oscillation (RO) pulsations" or "mode-beating (MB) pulsations."

External control parameters of the device are the laser and phase currents, $I_{DFB}$ and $I_P$, respectively. Varying these parameters, the device undergoes transitions between the above described regimes in a systematic way. As seen in Fig. 3, cycles of alternating self-pulsations and cw states appear in dependence on $I_P$ because of the phase-tuning property of this current. For a number of reasons, the behavior is not fully periodic. First, saturation sets in the $\phi$-$I_P$ relation at higher bias. Second, variation of $I_{DFB}$ shifts the emission wavelength changing $\phi$. However, most importantly, the feedback strength $K = \sqrt{R}\exp(-\alpha_P L_P)$ is also subject to change. Free-carrier absorption, coming into play at higher $I_P$, increases the losses ($\alpha_P$) in the feedback section. Studying the amplified spontaneous emission at transparency, we have found a reduction of $K$ from 0.3 to 0.1 in the $I_P$ range of Fig. 3. Note that the delay time $\tau = 2L_P/v_g$ ($v_g = c/3.8$: group velocity) is not measurably affected, either by $I_P$ or $I_{DFB}$. In the following paragraph, we demonstrate that two types of Hopf bifurcations underlie the transitions of the laser state.

A Hopf bifurcation is characterized by a pair of complex conjugated eigenvalues of the dynamical matrix moving across the imaginary axis yielding undamped oscillations. In the present case, all possible oscillations are driven by noise. When the damping of one of those oscillators approaches zero, a respective peak emerges in the power spectrum as a precursor of the bifurcation, whose position and width are direct measures of the complex eigenvalue.

First, we examine the RO pulsations (Fig. 4). When approaching the pulsation region from below, the onset of stable self-pulsations is indicated by a steep increase of the modulation degree at critical $I_P^c = 28.5$ mA. A well-resolved resonance, already present in the power spectrum below $I_P^c$, is a precursor of this transition. Its spectral width ($\Delta\nu$) undergoes a marked decrease towards the self-pulsation boundary. These findings are in full accord with a subcritical Hopf bifurcation. Time transients,

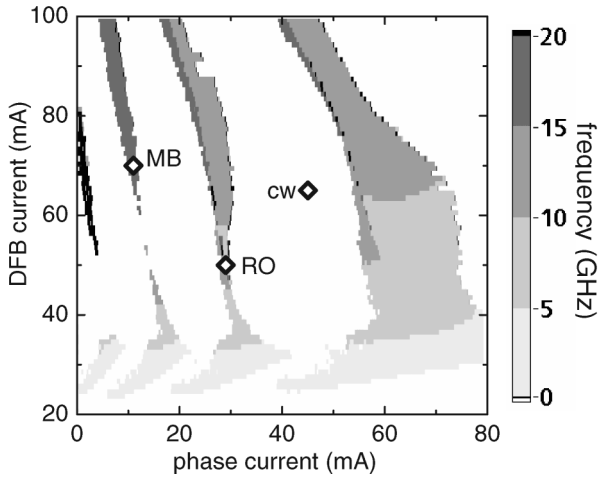


FIG. 3. Self-pulsation regions in the plane of external parameters $I_P$ and $I_{DFB}$. The grey levels code the frequency of the major peak in the power spectrum. White area: peak less than 5 dB above noise floor. Diamonds mark position, where the spectra of Fig. 2 and the horizontal cuts Figs. 4 and 5 are taken.

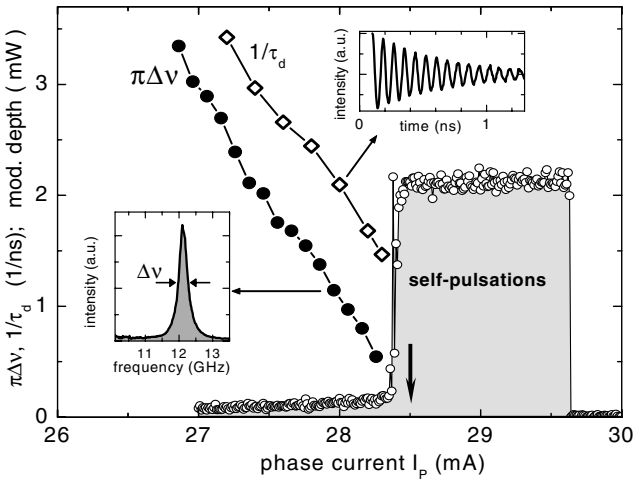


FIG. 4. Degree of modulation (small circles), resonance width (full circles), and damping rate (open circles) versus $I_P$ at the boundary of the RO self-pulsation. $I_{DFB} = 50$ mA. Arrow: spectra are shown in Fig. 2. Upper inset: time decay of relaxation oscillations. Lower inset: power spectrum.

recorded when the laser is disturbed below $I_P^c$ by an external optical pulse, reveal relaxation oscillations of 12 GHz frequency. This number is about 4 times larger than for similar lasers without feedback [10], but identical with the position of the resonance peak in the power spectrum. In addition, the damping rate ($1/\tau_d$) of the oscillations follows closely the slope of $\Delta\nu$. (The horizontal offset between the curves is due to a slight shift of the operation point by the optically injected carriers.) These findings confirm that undamped relaxation oscillations are indeed the origin of the RO-type laser state. The laser mode is destabilized by dispersive $Q$ switching mediated through gain-index coupling [11].

The onset of the MB pulsations is not sharp, but the modulation degree increases smoothly here (Fig. 5). The resonance in the power spectrum emerges again from a precursor, whose width declines rapidly when approaching the pulsation region. The MB pulsations are thus born in a supercritical Hopf bifurcation [6]. In contrast to the RO transition, the decay rates of the relaxation oscillations remain fast along this bifurcation, confirming that the origin of the MB pulsations is different. Both pulsations disappear by a jump to the next cavity mode, partly due to a homoclinic bifurcation. Excitability [9] and various kinds of hysteresis occur here. This will be detailed elsewhere.

Diverse bifurcations have been theoretically predicted for optical feedback lasers [6–8]. The above observations reveal a specific scenario that is analyzed now more closely. The longitudinal modes of the compound cavity, comprising DFB and feedback section, follow from the round-trip condition

$$q(\Omega, N)\exp(-i\Omega\tau) = K\exp(-i\phi), \tag{1}$$

where $N$ is the average carrier density in the laser and $\Omega$ denotes the complex mode frequency, measured relative to the Bragg resonance at transparency. The DFB enters here by its inverse amplitude reflectivity [12]

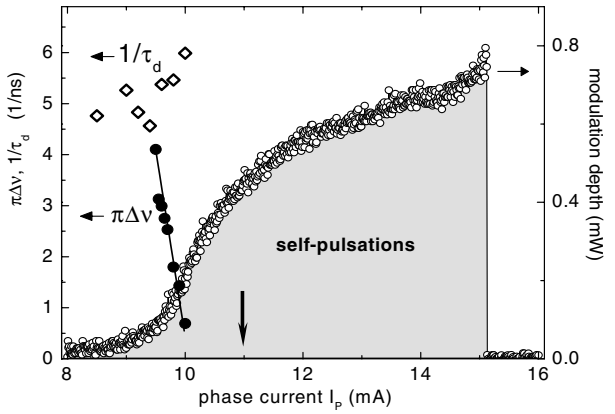


FIG. 5. Same as in Fig. 4 but for MB pulsations. $I_{DFB} = 70$ mA. Arrow: spectra are shown in Fig. 2.

$$q = \frac{i\gamma}{\kappa}\cot(\gamma L_{DFB}) - \frac{\beta}{\kappa} \tag{2}$$

with $\gamma^2 = \beta^2 - \kappa^2$ and the propagation constant

$$\beta(\Omega, N) = \frac{1}{2}[(i + \alpha_H)g'(N - N_{tr}) - \alpha_0] + \frac{\Omega}{v_g}. \tag{3}$$

The parameters involved ($\kappa = 130\ \mathrm{cm}^{-1}$; coupling coefficient of index grating, $\alpha_H = -5$; linewidth enhancement factor, $\alpha_0 = 25\ \mathrm{cm}^{-1}$; background absorption, $g' = 10^{-20}\ \mathrm{m}^2$; differential gain, including the transverse confinement factor, $N_{tr} = 10^{24}\ \mathrm{m}^{-3}$; carrier density at transparency level) have been deduced from independent measurements.

Figure 6, upper panel, depicts the solutions of Eq. (1) for real $\Omega$ by curves of constant $K$ and constant $\phi$ in the wavelength-density plane. Standard single-mode stability analysis [11] yields two types of instabilities: saddles in the region labeled "antimodes" and undamped relaxation oscillations in the small island denoted by "URO." The active mode of the solitary laser ($K = 0$) is represented by the vertex, where the equiphase lines move together. Those lines, not ending in the vertex, belong to other cavity modes. Curves of constant feedback strength are orbits $|\, q(\Omega, N)\,| = K$ around this vertex, the extension of which is an increasing function of $K$. At certain $K$, such an orbit touches the URO island. The island topology in the upper panel of Fig. 6 explains why

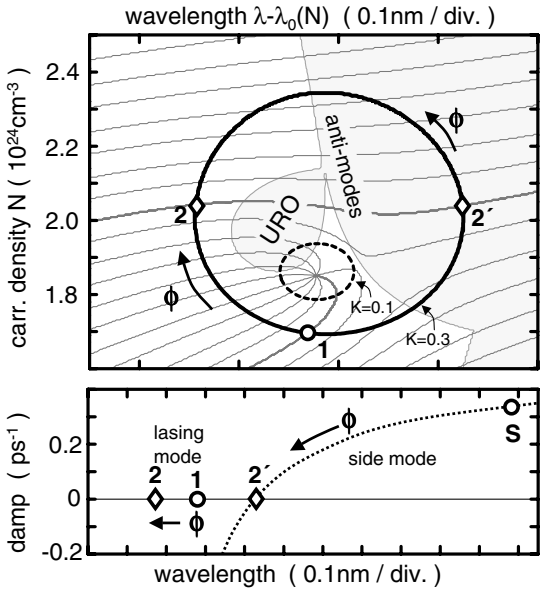


FIG. 6. Mode schema calculated from Eqs. (1)–(3). Upper panel: Curves of constant feedback ($K = 0.1$, dashed line; $K = 0.3$, solid line) and curves of constant phase (thin grey, 10 lines per phase period) in the wavelength-density plane. The carrier-induced shift $\lambda_0(N)$ is subtracted for clarity. Grey area: regions of instability. Lower panel: damping and wavelength of the active modes and first side modes. The side mode $S$ moves along the dashed line when changing the laser state from 1 to 2.

RO pulsations are found only in higher phase periods of $I_P$ (see Fig. 3), as $K$ is sufficiently reduced here. It is also consistent with the observation of similar Hopf bifurcations for longer cavities [3,5]. Undamped relaxation oscillations are hence a common feature of short and ultrashort cavities with weak feedback.

While the form of the orbit is independent of $\tau$, the delay controls the number of modes enclosed. For small $K$, it holds $\exp(i\Omega\tau) \approx 1$ along the orbit. Only one mode exists that rotates with $\phi$ clockwise around the orbit. However, variation of $\Omega\tau$ along extended orbits is associated with a change of $\phi$ by more than one period, thus enabling several modes. It is this interrelation between feedback delay and strength that gives rise to new dynamics, even though $\tau/\tau_R \ll 1$. The variation of $\phi$ is not monotonous along the orbit. The equiphase lines are tangential with the orbit, where it enters the antimode region. Pairs of modes appear or disappear here in saddle-node bifurcations. With increasing $\phi$, the stable modes move up on the left part of the loop, while the unstable antimodes do so on the right-hand side.

Stability of the laser state in the presence of more than one mode is beyond the analysis used so far. Therefore, Eq. (1) is solved at given $N$ for complex $\Omega$, where the imaginary part represents the mode damping. Let us consider a state 1 close to the minimum density of the orbit (○). In addition to the active mode, there are side modes of the compound cavity, all below threshold. When increasing $\phi$, 1 walks up until it reaches state 2 after one phase period (◇). Here, mode 2 and antimode $2'$ belong to the same $N$. The lower panel of Fig. 6 shows the damping along this path for the lasing mode and the side mode $S$ closest to threshold. While the lasing mode stays at threshold condition, the damping of $S$ decreases continuously and enters the negative range just above state 2. Here, the system becomes unstable and the laser switches back to state 1 with the same relative phase. However, before reaching instability, the side mode is only very weakly damped within a small interval of $\phi$. Here, both modes accommodate each other at a common density, and MB pulsations emerge in a Hopf bifurcation. This scenario is reminiscent of the bifurcation bridges predicted for long delay times [6]. The peculiar feature of the ultrashort cavity regime is the existence of only one antimode, yielding regular dynamics, whereas the pulse-package scenario [3] involves multiple antimodes. The device output is therefore qualitatively different. Pulse packages are pulse sequences with a repetition rate exactly given by the external cavity frequency $1/\tau$, amplitude-modulated with a frequency below $1/\tau_R$. The MB pulsations are not modulated and their frequency is by about 1 order of magnitude smaller than $1/\tau$, due to pulling of the side mode by the DFB resonance. The transition between both regimes is an interesting subject of future research. We note finally that the instability above state 2 is also a source of hysteresis. For decreasing $\phi$, state 1 moves to longer wavelengths and, in contrast to the forward phase, reaches the saddle-node bifurcation. Here, the laser switches to the only stable state of the same $\phi$ on the left part of the orbit, about three phase grids below state 2. We have, indeed, experimentally observed respective wavelength jumps and power drops in low phase periods.

In conclusion, our study has revealed specific routes of self-organization in lasers with ultrashort optical feedback. As the result of Hopf bifurcations, regular self-pulsations of high stability and well-defined frequencies emerge. The short-feedback laser exhibits also a variety of further dynamical phenomena, as will be reported soon.

This work was supported by the Deutsche Forschungsgemeinschaft in the framework of Sfb 555. The authors thank Bernd Sartorius for providing the device.

*Electronic address: henne@physik.hu-berlin.de

[1] H. Haken, *Laser Theory* (Springer-Verlag, Berlin, 1986).
[2] R. Lang and K. Kobayshi, IEEE J. Quantum Electron. **16**, 347 (1980).
[3] T. Heil, I. Fischer, W. Elsäßer, B. Krauskopf, K. Green, and A. Gavrielides, Phys. Rev. E **67**, 066214 (2003); T. Heil, I. Fischer, W. Elsäßer, and A. Gavrielides, Phys. Rev. Lett. **87**, 243901 (2001).
[4] A. Tager and B. Elenkrieg, IEEE J. Quantum Electron. **29**, 2886 (1993); A. Tager and K. Petermann, IEEE J. Quantum Electron. **30**, 1553 (1994).
[5] A. Hohl and A. Gavrielides, Phys. Rev. Lett. **82**, 1148 (1999).
[6] D. Pieroux *et al.*, Phys. Rev. Lett. **87**, 193901 (2001); B. Haegeman *et al.*, Phys. Rev. E **66**, 046216 (2002).
[7] M. Wolfrum and D. Turaev, Opt. Commun. **212**, 127 (2002).
[8] J. Sieber, SIAM J. Appl. Dyn. Sys. **1**, 248 (2002).
[9] H-J. Wünsche, O. Brox, M. Radziunas, and F. Henneberger, Phys. Rev. Lett. **88**, 023901 (2002).
[10] An enhanced frequency at the Hopf bifurcation as well as its slight decrease with the pulsation amplitude are typical features of lasers with dispersive feedback [11]. In the present device, the dispersion due to the ultrashort feedback delay is sufficient to cause these effects.
[11] Vasile Z. Tronciu, H-J. Wünsche, J. Sieber, K. Schneider, and F. Henneberger, Opt. Commun. **182**, 221 (2000).
[12] John E. Carroll, J. E. A. Whiteaway, R. G. S. Plumb, and D. Plumb, *Distributed Feedback Semiconductor Lasers* (IEE Publishing, London, U.K., 1998).